Journal of Alloys and Compounds 498 (2010) 102–106

Contents lists available at ScienceDirect

Journal of Alloys and Compounds

journal homepage: www.elsevier.com/locate/jallcom

Correlation between the temperature dependence of yield stress and the nature of solute distribution in Cu–Ni solid solutions

Muhammad Zakria Butt*, Farah Aziz, Dilawar Ali

Department of Physics, University of Engineering and Technology, G T Road, Lahore 54890, Pakistan

ARTICLE INFO

Article history:
Received 17 November 2009
Received in revised form 26 February 2010
Accepted 14 March 2010
Available online 18 March 2010

Keywords:
Cu–Ni alloys
Yield stress
Temperature dependence
Nature of solute distribution

ABSTRACT

Nature of solute distribution in copper single crystals alloyed with 0–100 at.% Ni has been investigated via temperature dependence of the yield stress. The composition–property diagram developed and interpreted in terms of the kink-pair nucleation model of flow stress in solid–solution crystals shows that the solute distribution is statistically random in Cu–Ni single crystals with solute concentration $c \leq 14$ at.% Ni, and is non-random for c between 14 and 50 at.% Ni. Similarly, the solute distribution is statistically random in Ni–Cu single crystals with $c \leq 20$ at.% Cu, and deviation from statistically random distribution of solute occurs for all other values of c up to 50 at.% Cu.

1. Introduction

The physical, functional, electrical and mechanical properties of crystalline materials are closely linked to the microstructural developments [1–11] which occur in the lattice. This is true for both solid–solution as well as nominally pure element crystals. For instance, solute segregation to partial dislocations [2–5] and stacking faults [6] as well as local ordering (whether short-range order or clustering) of solute atoms [7–9] in single-phase binary and ternary alloys play an important role in this regard. So is the case with the nominally pure metals [10–12] in which migration of point defects, e.g. residual gaseous and metallic impurity atoms and above-equilibrium vacancies, etc., to the cores of dislocations modify their mechanical properties.

As far as alloys are concerned, the non-random distribution of solute atoms has a marked effect on the principal features of solid–solution hardening, such as the temperature and concentration dependence of yield stress and associated activation volume [13–18], the stress dependence of activation volume [19], and the phenomenon of stress equivalence [9,20,21]. So is the case for other mechanical properties of solid–solution crystals, such as work-hardening rate [22], internal friction [23], creep [22,24], stress relaxation [25,26], and strain rate sensitivity of flow stress [27]. To explore the relationship between the temperature dependence of critical resolved shear stress (CRSS) of solid–solution crystals and the nature of solute distribution, Butt and co-workers [13–16] carried out investigations with a number of copper-based binary alloy systems. They found that the CRSS τ of Cu–Zn [13], Cu–Al [14], Cu–Ge [15] and Cu–Mn [16] varies with the deformation temperature T in accord with the relation:

$$\ln \tau = A - BT \quad (1)$$

in the temperature domain where diffusional processes in the crystal are dormant. Here A and B are positive constants values of which depend on the solute concentration c, and can be determined from the experimental τ–T data plotted in semi-logarithmic coordinates by least-squares fitting method. For each solid–solution system referred to, the experimental value of constant B [$=-\mathrm{d}\ln\tau/\mathrm{d}T$], which is a measure of the degree of temperature dependence of CRSS, decreases as solute concentration c increases till a critical value c_m, and then increases with further increase in c till the first solubility limit. This indicates that the modes of solute distribution in the crystals with solute concentration c below and above c_m are not the same. The values of c_m determined in this manner for copper-based alloys were found to be 27 at.% Zn, 7 at.% Al, 5 at.% Ge and 1 at.% Mn, which are well below the respective first solubility limit of Zn, Al, Ge and Mn in copper lattice. This behaviour was also observed in the case of non-metallic KBr–KCl solid–solution crystals containing 8–41 mol% KCl with $c_m = 35$ mol% KCl [28] and KCl–KBr solid–solution crystals containing 9–45 mol% KBr with $c_m = 35$ mol% KBr [29].

One can readily gather from the standard equilibrium phase diagrams for copper-based binary alloys that the solubility of Zn, Al, Ge and Mn in Cu to form single-phase binary solid–solution is limited, whereas Ni can be dissolved in Cu to any extent. Hence it was considered more instructive to extend the above cited investiga-

* Corresponding author. Tel.: +92 42 99029204; fax: +92 42 99250202.
E-mail address: mzbutt49@yahoo.com (M.Z. Butt).

0925-8388/$ – see front matter © 2010 Elsevier B.V. All rights reserved.
doi:10.1016/j.jallcom.2010.03.122

tions carried out with copper-based alloys with limited solubility range to the one with complete solubility range. The mode of solute distribution in Cu–Ni solid–solution crystals with solute content in the range 0–100 at.% Ni was thus explored in the present work by constructing a composition–property diagram within the frame work of the KPN model [30,31] of solid–solution hardening. The wealth of data obtained by Suzuki [32] with Cu–Ni alloy single crystals (c = 5–95 at.% Ni) annealed at 1000 °C for a few days or at 1050 °C for two weeks prior to their deformation in tension at rather slow strain rate in the temperature range 20–373 K, was considered for this purpose. Analysis was confined to the data pertaining to only those crystals which did not change their orientation during annealing treatment. The τ–T data obtained by Kamada and Yoshizawa [33] with relatively less concentrated Cu–Ni alloy single crystals (c = 0.5–5.3 at.% Ni) annealed at 1000 °C for 48 h and furnace cooled down to room temperature before tensile testing at a strain rate of 6×10^{-5} s^{-1} in the temperature range 1.6–315 K, was also taken into account.

2. The KPN model

In the KPN model of flow stress in solid–solution crystals, Butt and Feltham [30,31] visualized yielding to occur as a consequence of the breakaway of edge-dislocation segments simultaneously from several, randomly distributed, closely spaced, solute–atom pinning points. These barriers were regarded as "smeared out" over the segment length in a manner somewhat similar to the "kink-pair mode of escape" of screw dislocations from a Peierls barrier [34]. Pinning of screw dislocations with solute atoms was considered too weak by comparison to result in effective barriers to glide. The CRSS τ of the solid–solution crystals, which depends on the deformation temperature T and the solute concentration c, is then given by the relation [30,31]

$$\tau = \tau_o \exp\left(-\frac{mkT}{W_o}\right) \quad (2)$$

which is valid over the temperature range where no diffusional effects occur in the crystal. It should be noted that Eq. (1) is an alternative form of Eq. (2) with $A = \ln \tau_o$ and $B = (mk/W_o)$. Here τ_o is the CRSS as $T \to 0$ K, W_o is the interaction energy between the edge-dislocation segment of length L_o and the solute atoms close to it, $m = \ln(\dot{\gamma}_o/\dot{\gamma})$ is a constant equal to 25 ± 2.3 for the deformation rate $\dot{\gamma}_o = 10^{-3} - 10^{-5}$ s^{-1} and the pre–exponential factor $\dot{\gamma}_o = 10^7\, s^{-1}$, and k is the Boltzmann constant. In terms of the microscopic slip parameters, $\tau_o = 4Uc^{1/2}/nb^3$ and $W_o = n(Uc^{1/2}Gb^3)^{1/2}$, where G is the shear modulus, b is the length of the Burgers vector, U represents the average binding energy of a solute atom with the edge dislocation, nb is the maximum critical height of the bulge, somewhat akin to a kink-pair, in the process of its nucleation after the initial breakaway of an edge-dislocation segment simultaneously from several solute-atom pinning points to the saddle configuration. The value of n is expected to be 4–6 in the case of concentrated face-centred cubic and hexagonal close-packed alloy crystals with low intrinsic lattice friction whereas it would be somewhat smaller, i.e. 1–2, for body-centred cubic alloy crystals with high intrinsic lattice friction.

It is worthy of note that the value of U is numerically less than the maximum binding energy U_{max} [35] of a solute atom with the edge dislocation arising from the size-misfit $\delta = (1/b)(db/dc)$ and modulus-mismatch $\eta = (1/G)(dG/dc)$ of solute in the solvent or host lattice. It is so because a "partially flexible" dislocation lying in the glide plane containing a concentration of randomly dispersed solute atoms cannot be "fully pinned" individually at all the solute atoms along its length.

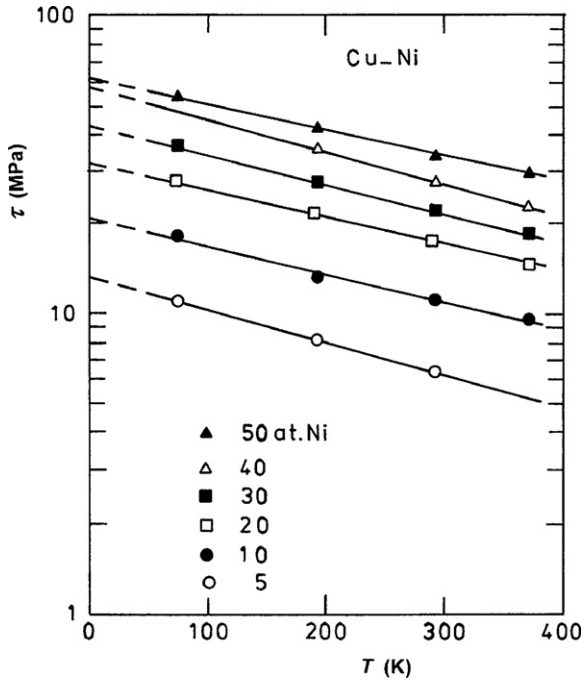

Fig. 1. Log–linear relationship between the CRSS τ and the deformation temperature T for Cu–Ni single crystals. Data points were taken from Suzuki [32].

3. Data analysis

The data points in Fig. 1 denote the values of CRSS τ of Cu single crystals alloyed with 5–50 at.% Ni in the temperature range 77–373 K, while those in Fig. 2 pertain to Ni single crystals containing 5–40 at.% Cu for the deformation temperatures between 60 and 373 K. The measured CRSS values in both the cases are due to Suzuki [32]. The straight lines were drawn through the date points for a given solute concentration by least-squares fitting method

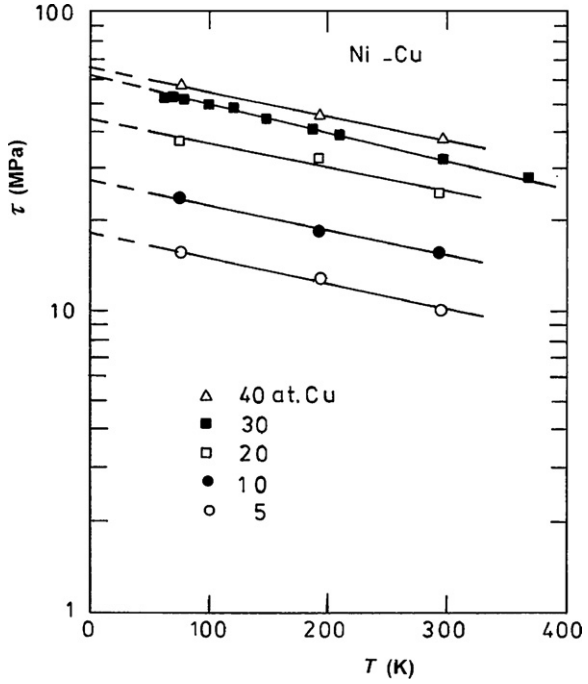

Fig. 2. Log–linear relationship between the CRSS τ and the deformation temperature T for Ni–Cu single crystals. Data points were taken Suzuki [32].

Table 1
Values of constants A and B in Eq. (1) along with linear correlation coefficient r and standard deviation SD for Cu–Ni alloys. Slip nucleation parameters of the KPN model were evaluated from the theoretical formulae on using (a) $G = 4.5 \times 10^4$ MPa, $b = 0.2556$ nm and $Gb^3 = 4.7$ eV for $c = 0.5$–40 at.% Ni in Cu lattice, (b) $G = 6.0 \times 10^4$ MPa, $b = 0.2524$ nm and $Gb^3 = 6.0$ eV for $c = 50$ at.% Ni in Cu lattice, and (c) $G = 7.5 \times 10^4$ MPa, $b = 0.2492$ nm and $Gb^3 = 7.2$ eV for $c = 5$–40 at.% Cu in Ni lattice.

c	A	$B\,(10^{-3})$	r	SD	τ_o (MPa)	W_o (eV)	n	U (meV)	$L_o\,(b)$	$v_o\,(b^3)$
0.5 at.% Ni	0.952	3.468	−0.990	0.039	2.6	0.621	10.7	10.1	861	2303
1.3	1.556	3.384	−0.990	0.044	4.7	0.637	8.9	9.6	584	1299
3.2	2.170	2.781	−0.999	0.021	8.8	0.775	8.2	10.6	410	841
5.3	2.382	2.593	−0.996	0.020	10.8	0.831	8.0	10.0	365	730
5 at.% Ni	2.585	2.547	−0.999	0.004	13.3	0.846	7.6	11.8	321	610
10	3.040	2.163	−0.994	0.039	20.9	0.996	7.3	12.5	251	458
20	3.474	2.109	−0.999	0.014	32.3	1.021	6.4	12.1	189	302
30	3.767	2.314	−0.999	0.017	43.2	0.931	5.5	11.3	151	208
40	4.060	2.561	−0.999	0.012	58.0	0.841	4.6	11.2	119	137
50	4.149	2.109	−0.999	0.010	63.4	1.021	4.8	10.8	135	162
5 at.% Cu	2.912	1.983	−0.997	0.025	18.4	1.086	7.2	14.2	342	612
10	3.316	1.878	−0.998	0.013	27.5	1.147	6.5	13.7	266	432
20	3.770	1.715	−0.973	0.060	43.4	1.256	5.9	13.9	202	300
30	4.096	2.105	−0.998	0.013	60.1	1.023	4.6	12.3	152	177
40	4.178	1.855	−0.999	0.012	65.2	1.161	4.9	12.3	150	185

in accord with the model Eq. (1), which predicts a linear relationship between $\ln\tau$ and T. The values of positive constants A and B, along with linear correlation coefficient r and standard deviation SD, obtained in each case are given in Table 1.

Similarly, Fig. 3 depicts the temperature dependence of the CRSS τ of Cu single crystals with solute content 0.5–5.3 at.% Ni between 50 and 315 K in log–linear coordinates. Date points denote the CRSS values measured by Kamada and Yoshizawa [33]. The straight line fitted to the data points for a given solute concentration by least-squares fitting method provides the values of positive constants A and B in Eq. (1). These values together with those of linear correlation coefficient r and standard deviation SD obtained for each alloy concentration are also given in Table 1. It should be noted that the CRSS values below 50 K were not included in Figs. 1–3 due to the anomalous τ–T dependence observed at rather low temperatures [32,33], and were analyzed elsewhere [36].

Using the values of A and B, one gets the values of τ_o (=exp A) and W_o (=mk/B) given in Table 1. Knowing τ_o and W_o, one can evaluate the microscopic parameters n and U for the complete Cu–Ni alloy system on substituting appropriate values of c, G and b in the relations [30,31]

$$n^3 = \left(\frac{W_o}{Gb^3}\right)^2 \left(\frac{4G}{\tau_o}\right) \tag{3}$$

$$U = \frac{W_o^2}{Gb^3 n^2 c^{1/2}} \tag{4}$$

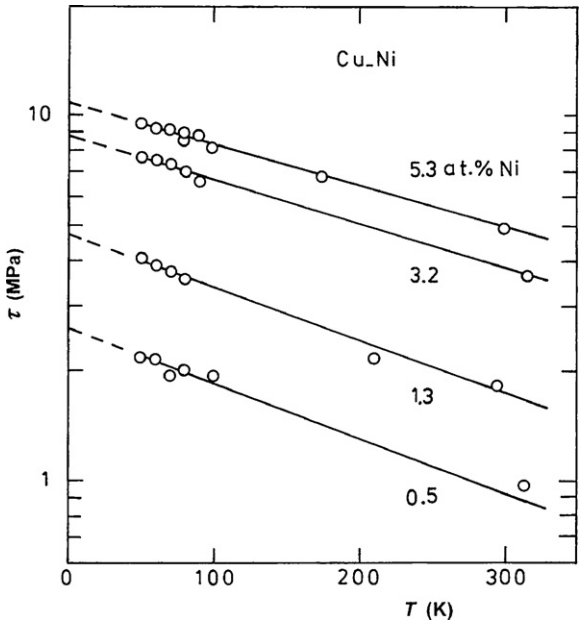

Fig. 3. Log–linear relationship between the CRSS τ and the deformation temperature T for Cu–Ni single crystals. Data points were taken from Kamada and Yoshizawa [33].

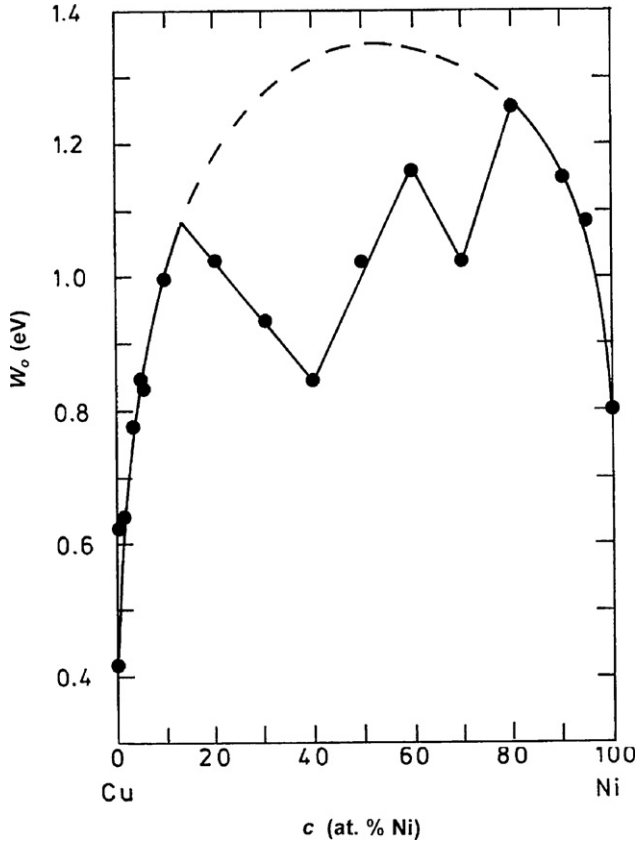

Fig. 4. Dependence of the KPN model parameter W_o (=mk/B) on the solute concentration c for the complete range of Cu–Ni alloy system in linear–linear representation.

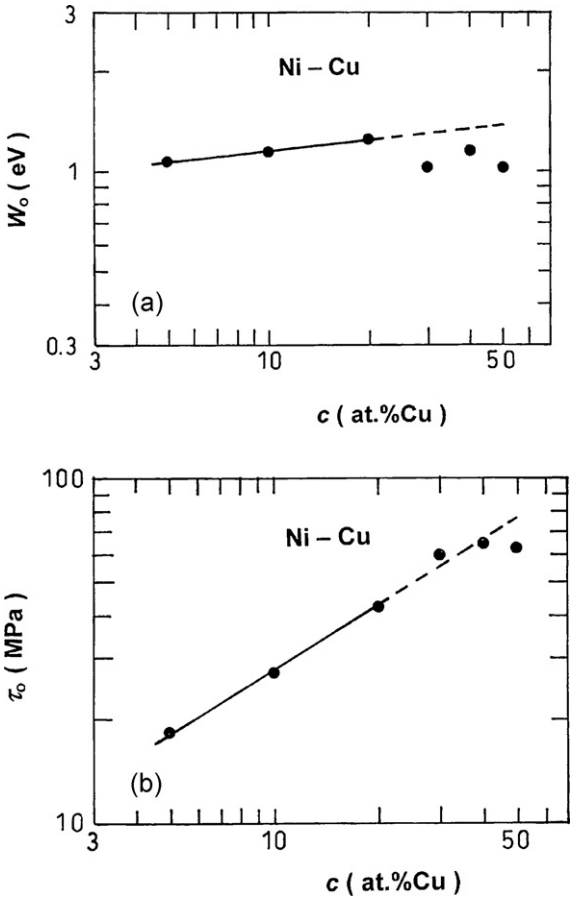

Fig. 5. Relationship between the solute concentration c and the KPN model parameters (a) W_o and (b) τ_o for Ni–Cu alloys in logarithmic coordinates.

derived from the model expressions $\tau_o = 4Uc^{1/2}/nb^3$ and $W_o = n(Uc^{1/2}Gb^3)^{1/2}$. The length of the edge-dislocation segment

$$L_o = b\left(\frac{4Gn}{\tau_o}\right)^{1/2} \tag{5}$$

involved in the unit activation process of yielding at $T \to 0$ K, and the associated activation volume [30,31]

$$v_o = \left(\frac{1}{4}\right) nL_o b^2 \tag{6}$$

were also evaluated, and are listed in Table 1 along with the values of n and U. These values are of the right order of magnitude for the glide of edge-dislocation segments in solid–solution crystals, as anticipated in the KPN model.

To detect any heterogeneity of solute distribution in the alloy crystals we shall now examine the concentration dependence of the parameter $W_o(=mT/B)$ on the solute concentration c for the complete Cu–Ni alloy system. The points in Fig. 4 denote the values of W_o for Cu–Ni alloy single crystals containing 0.5–95 at.% Ni given in Table 1, while those for pure Cu and pure Ni crystals were taken from Feltham and Kauser [37] and Butt and Sattar [18], respectively. One can readily note that in the case of Cu–Ni alloys, W_o increases monotonically with c up to about 14 at.% Ni in accord with the model prediction, i.e. $W_o \propto c^{1/4}$, which is based on statistically random distribution of solute atoms. However, as c increases beyond $c_m \approx 14$ at.% Ni, W_o decreases till 40 at.% Ni by about 30%, indicating a departure from the random solute distribution. Similarly, W_o increases monotonically with c up to about 20 at.% Cu in the case of Ni–Cu alloy single crystals, and later on variation of W_o with c becomes irregular till 50 at.% Cu such that the experimental values of W_o are lower than the theoretically expected ones ($W_o \propto c^{1/4}$) encompassed by the broken W_o–c curve in Fig. 4. It means that the distribution of Cu solute atoms in the Ni host lattice is statistically random below $c_m \approx 20$ at.% Cu, and beyond that it is non-random.

Thus in Cu–Ni alloy system (c = 0–100 at.% Ni), the distribution of solute atoms is non-random for the solute concentrations between 14 and 80 at.% Ni, whereas for all other values c, it is statistically

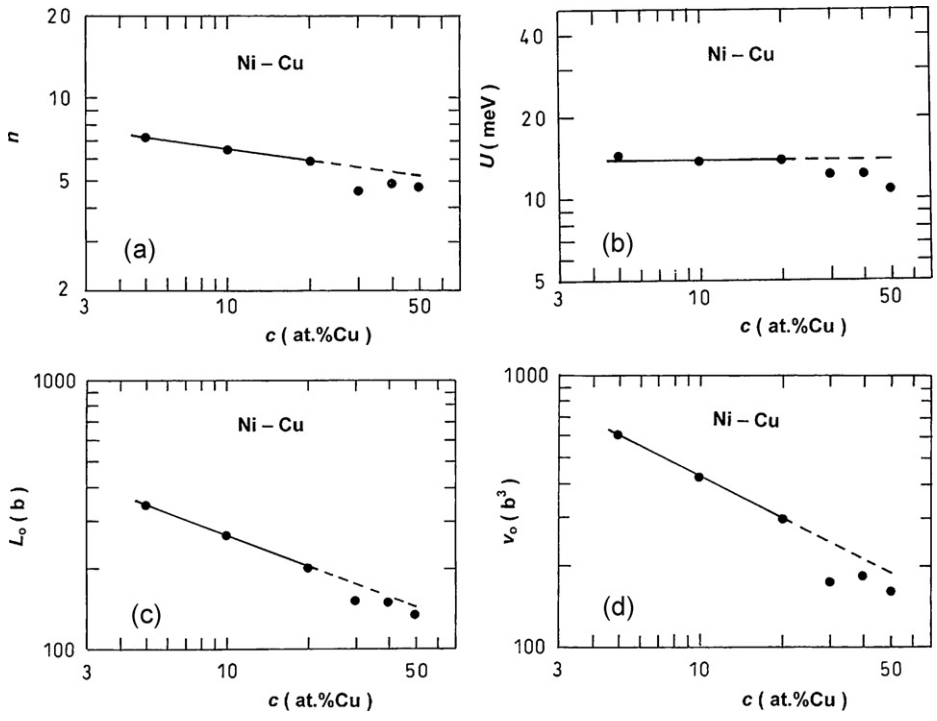

Fig. 6. Relationship between the solute concentration c and the KPN model parameters (a) n, (b) U, (c) L_o and (d) v_o for Ni–Cu alloys in logarithmic coordinates.

Table 2
Numerical values of constants C and D in Eq. (7) for a linear relationship between $\ln P$ and $\ln c$, along with linear correlation coefficient r and standard deviation SD, for Ni–Cu ($c \leq 20$ at.% Cu) and Cu–Ni ($c \leq 14$ at.% Ni) alloy single crystals.

Alloy	P	C	D	r	SD	c range
Ni–Cu	W_o	0.39	+0.11	+0.989	0.015	5–20 at.% Cu
	τ_o	4.76	+0.62	+0.999	0.022	
	n	1.54	−0.14	−0.999	0.002	
	U	2.60	−0.01	−0.654	0.016	
	L_o	4.70	−0.38	−0.999	0.009	
	ν_o	4.88	−0.51	−0.999	0.006	
Cu–Ni	W_o	0.31	+0.16	+0.963	0.055	0.5–14 at.% Ni
	τ_o	4.55	+0.68	+0.993	0.099	
	n	1.69	−0.12	−0.977	0.033	
	U	2.61	+0.07	+0.697	0.085	
	L_o	4.62	−0.40	−0.993	0.057	
	ν_o	4.92	−0.53	−0.992	0.080	

random. Literature survey shows that there is a strong tendency of dendrite formation during crystal growth in many important commercial alloys [38–45]. For instance, dendrites have been observed in rather concentrated Cu–Ni solid–solution crystals with c = 20, 30, 50 and 75 at.% Ni [42–45]. Also, the phenomenon of solute trapping in the case of rapid solidification of the alloys [46] results in a cored structure with regions of different chemical compositions. In fact, the heterogeneity of the solute distribution due to dendritic growth or concentration gradient due to solute trapping in rather concentrated Cu–Ni alloy crystals is removed during their heat treatment at 1000 °C for a prolonged period of time [32,33]. However, natural ageing of the annealed specimens prior to their deformation allows segregation of solute atoms to some extent in rather concentrated solid–solutions. Had these alloy crystals been quenched after heat treatment in order to freeze the statistically random solute distribution achieved during annealing, and not allowed to age at room temperature prior to tensile tests, the points denoting W_o values would have been on the broken W_o–c curve (Fig. 4) between 14 and 80 at.% Ni. This can, however, be confirmed only by further experimentation on the above lines in future work.

To substantiate the observed correlation between W_o and c (Fig. 4) further, we shall now examine the concentration dependence of the macroscopic parameters W_o and τ_o (Fig. 5) as well as that of the microscopic parameters n, U, L_o and ν_o (Fig. 6). The points in Figs. 5 and 6 denote the values of the model parameters referred to above for Ni–Cu alloy single crystals (c = 5 to 50 at.% Cu), taken from Table 1, as function of solute concentration c in logarithmic coordinates. The straight line drawn through data points by least-squares fitting method for c up to 20 at.% Cu in each case, is represented by the mathematical expression:

$$\ln P = C + D \ln c \tag{7}$$

Here P stands for the model parameters under investigation, and the numerical values of constants C and D, along with linear correlation coefficient r and standard deviation SD, are given in Table 2. However, the data points for $c > 20$ at.% Cu in Figs. 5 and 6 show marked deviation from the straight line encompassed by Eq. (7) for $c \leq 20$ at.% Cu in all the cases, which again indicates that the mode of solute distribution in Ni–Cu alloy single crystals with $c \leq 20$ at.% Cu is different from that for $c > 20$ at.% Cu.

Finally, reference to Eq. (7) together with the value of constant D for the model parameter W_o given in Table 2, shows that $W_o \propto c^{0.11}$, whereas the KNP model predicts $W_o \propto c^{0.25}$ with the stricture that G, b, n and U are independent of c. The difference in the observed and predicted values of the exponent, i.e. 0.11 and 0.25, respectively, can be accounted for in terms of the observed weak c-dependence of the microscopic parameters n and U. Assuming G and b are independent of solute concentration c, we can readily note (Table 2) that U is almost independent of c and $n \propto c^{-0.14}$ so that $W_o \propto nc^{0.25} \propto c^{0.11}$. Similarly, the difference in the observed ($\tau_o \propto c^{0.62}$) and predicted ($\tau_o \propto c^{0.50}$) c-dependence of τ_o is accounted for on noting that $\tau_o \propto n^{-1}c^{0.5} \propto c^{0.64}$. Moreover, the observed c-dependence of L_o and ν_o, i.e. $L_o \propto c^{-0.38}$ and $\nu_o \propto c^{-0.51}$, can be accounted for with reference to Eqs. (5) and (6) together with $n \propto c^{-0.14}$, which predict $L_o \propto nc^{-0.25}$ and $\nu_o \propto n^2c^{-0.25}$, respectively. On the same lines, one can also account for the observations in relation to the c-dependence of W_o, τ_o, n, U, L_o and ν_o (Table 2) for Cu–Ni alloys with $c < 14$ at.% Ni.

4. Conclusions

From the composition–property diagram developed in terms of the KPN model of solid–solution hardening, we conclude that the temperature dependence of the CRSS of the whole Cu–Ni solid–solution system (c = 0–100 at.% Ni) depends not only on the solute concentration but also on the nature of solute distribution. The solute distribution is statistically random in the Cu–Ni alloy single crystals for $c \leq 14$ at.% Ni and for $c \geq 80$ at.% Ni. However, for all other values of the solute concentration c between 14 and 80 at.% Ni, deviation from statistically random distribution of solute occurs in the Cu–Ni alloy crystals.

References

[1] R.J. Arsenault, Mater. Charact. 32 (1994) 275–286.
[2] A. Varschavsky, E. Donoso, Mater. Lett. 31 (1997) 239–245.
[3] A. Varschavsky, E. Donoso, J. Therm. Anal. 50 (1997) 533–545.
[4] A. Varschavsky, E. Donoso, J. Therm. Anal. 48 (1997) 1229–1248.
[5] A. Varschavsky, E. Donoso, Mater. Sci. Eng. A 251 (1998) 208–215.
[6] A. Varschavsky, Scr. Metall. 9 (1975) 391–397.
[7] V.V. Demirskiy, S.N. Komnik, V.I. Startsev, Phys. Met. Metall. 46 (1978) 151–158.
[8] P. Ruf, D. Koss, Phil. Mag. 30 (1974) 1319–1326.
[9] C. Schwink, T. Wille, Scr. Metall. 14 (1980) 1093–1100.
[10] M.Z. Butt, A.Q. Jakhar, H. Aslam, Phys. Status Solidi A 176 (1999) 877–884.
[11] M.Z. Butt, M. Zubair, I. ul-Haq, J. Mater. Sci. 35 (2000) 6139–6144.
[12] F. Bashir, M.Z. Butt, J. Mater. Sci. 42 (2007) 7801–7805.
[13] M.Z. Butt, I.M. Gharui, Phys. Status Solidi A 107 (1988) 187–195.
[14] M.Z. Butt, Z. Rafi, J. Mater. Sci. Lett. 10 (1991) 309–312.
[15] M.Z. Butt, M. Noshi, F. Bashir, Cent. Eur. J. Phys. 6 (2008) 834–842.
[16] M.Z. Butt, M.A. Khan, Phys. Status Solidi A 113 (1989) K189–K193.
[17] M.Z. Butt, J. Mater. Sci. Lett. 7 (1988) 879–880.
[18] M.Z. Butt, U. Sattar, J. Mater. Sci. Lett. 20 (2001) 759–761.
[19] T. Wille, W. Gieseke, C. Schwink, Acta Metall. 35 (1987) 2679–2693.
[20] M.Z. Butt, M.A. Shami, J. Mater. Sci. 23 (1988) 2661–2665.
[21] M.Z. Butt, J. Phys: Condens. Matter 2 (1990) 5797–5808.
[22] P. Feltham, G.J. Copley, Acta Metall. 8 (1960) 542–550.
[23] L. Guillet, in: N.F. Mott (Ed.), Report of a Conference on the Strength of Solids, The Physical Society, London, 1948, pp. 116–119.
[24] P. Feltham, G.J. Copley, Phil. Mag. 5 (1960) 649.
[25] P. Feltham, J. Inst. Metals 89 (1960–1961) 210–214.
[26] M.Z. Butt, M.S. Khiliji, J. Alloys Compd. 479 (2009) 252–256.
[27] R.C. Picu, G. Vincze, J.J. Gracio, F. Barlat, Scr. Metall. 54 (2006) 71–75.
[28] A. Asif, M.Z. Butt, J. Mater. Sci. 42 (2007) 2862–2866.
[29] A. Asif, M.Z. Butt, Phil. Mag. 87 (2007) 1811–1820.
[30] M.Z. Butt, P. Feltham, Acta. Metall. 26 (1978) 167–173.
[31] M.Z. Butt, P. Feltham, J. Mater. Sci. 28 (1993) 2557–2576.
[32] H. Suzuki, in: P.O. Kettunen, T.K. Lepisto, M.E. Lehtonen (Eds.), Strength of Metals and Alloys (ICSMA 8), vol. 2, Pergamon Press, Oxford, 1988, pp. 573–578.
[33] K. Kamada, I. Yoshizawa, J. Phys. Soc. Jpn. 31 (1971) 1056–1068.
[34] P. Feltham, J. Phys. D: Appl. Phys. 2 (1969) 377–382.
[35] I. Saxl, Czech. J. Phys. B23 (1973) 381–392.
[36] M.Z. Butt, F. Aziz, Phil. Mag. Lett. 87 (2007) 915–922.
[37] P. Feltham, N. Kauser, Phys. Status Solidi A 117 (1990) 135–140.
[38] W. Kurz, D.J. Fisher, Fundamentals of Solidification, Trans Tech, Aedermannsdorf, Switzerland, 1989.
[39] R. Trivedi, W. Kurz, Int. Mater. Rev. 39 (1994) 49–74.
[40] C. Huang, M.E. Glicksman, Acta Metall. 29 (1981) 701–715.
[41] C. Huang, M.E. Glicksman, Acta Metall. 29 (1981) 717–734.
[42] Q. Wang, M.Z. Ma, Q. Jing, G. Li, L. Qi, X.-Y. Zhang, W.-K. Wang, R.-P. Liu, Chin. Phys. Lett. 25 (2008) 3808–3810.
[43] J.F. Li, Y.H. Zhou, G.C. Yang, Mater. Sci. Eng. A 277 (2000) 161–168.
[44] J.F. Li, G.C. Yang, Y.H. Zhou, Mater. Res. Bull. 33 (1998) 141–148.
[45] J.F. Li, Y.C. Liu, Y.L. Lu, G.C. Yang, Y.H. Zhou, J. Cryst. Growth 192 (1998) 462–470.
[46] N.A. Ahmad, A.A. Wheeler, W.J. Boettinger, G.B. McFadden, Phys. Rev. E 58 (1998) 3436–3450.